A Persistent Carbenium Ion on the Methanol-to-Olefin Catalyst HSAPO-34: Acetone Shows the Way

Weiguo Song,[†] John B. Nicholas,*[,‡] and James F. Haw*[,†]

Loker Hydrocarbon Research Institute and Department of Chemistry, University of Southern California, University Park, Los Angeles, California 90089-1661, and the Environmental Molecular Sciences Laboratory, Pacific Northwest National Laboratory, P.O. Box 999, Richland, Washington 99352

Received: November 9, 2000; In Final Form: January 29, 2001

In situ ^{13}C NMR with both CAVERN and pulse−quench methods was used to understand the chemistry of acetone on the silico-aluminophosphate catalyst HSAPO-34. The isotropic shift of [2-^{13}C]acetone shows that most of the acid sites on this catalyst are weaker than those on aluminosilicate zeolites, but a minority site was resolved with a shift higher than that on zeolite HZSM-5. At elevated temperatures, acetone dimerized to diacetone alcohol and dehydrated to mesityl oxide. Mesityl oxide cracked in the presence of water to acetic acid and isobutylene. Trimerization of butenes formed a significant amount of a persistent carbenium ion with unusual spectroscopic properties, and this is proposed to be the heptamethylcyclopentenyl cation, the first observation of a persistent carbenium ion on a SAPO catalyst. Chemical shift calculations at the GIAO-MP2 level revealed a discrepancy for one signal of the proposed cation but ruled out an alternative assignment. Methylaromatic formation coincided with cyclopentenyl cation synthesis, supporting a mechanistic proposal for aromatic synthesis on zeolites. Conventional flow reactor studies revealed a high selectivity for C_4 olefins and rapid deactivation with acetone as feed. The results of this investigation are interpreted in the context of methanol-to-olefin (MTO) chemistry on HSAPO-34.

The catalytic conversion of methanol to olefins (MTO)[1] is a major emerging chemical technology and the key step in the conversion of natural gas to polyolefins by otherwise mature chemistry. The most promising catalysts for commercial trials are solid acids based on silico-aluminophosphates of the chabazite (CHA) structure, most simply HSAPO-34.[2] The topology of this catalyst is characterized by cages of ca. 1.0 nm by 0.7 nm diameter that are interconnected through 8-ring windows of ca. 0.38 nm in diameter. Thus, reactants such as methanol and dimethyl ether and products such as ethylene, propene, and 1-butene may freely diffuse through active catalysts, but larger molecules, even those with kinetic diameters comparable to that of isobutane, are not adsorbed.

Applied research in MTO catalysis is directed toward increasing both ethylene selectivity and catalyst lifetime, and this has motivated basic research into the mechanisms of olefin synthesis and catalyst deactivation. In a recent publication,[3] we used pulse−quench reactors to study MTO chemistry on HSAPO-34. Gas chromatographic analysis, alone (GC) and coupled with mass spectrometry (GC-MS), of the volatile products confirmed the existence of a kinetic induction period on this catalyst. Only a modest conversion of methanol to hydrocarbons was observed following the *first* pulse of methanol onto a fresh catalyst, but essentially 100% conversion was obtained for a *second*, identical pulse applied a few minutes later. Furthermore, GC-MS showed that when the first pulse was [^{13}C]methanol and the second pulse was [^{12}C]methanol, the predominant isotopomer of ethylene in the product stream had one carbon of each isotope. We used ^{13}C MAS NMR analysis of quenched samples from these reactor studies to understand the changes occurring on HSAPO-34 following first exposure of methanol to create a working catalyst. Those measurements showed that methylbenzenes self-assemble in the cages of HSAPO-34 in the first few seconds following methanol exposure and that these "organic reaction centers" are part of the active site of a working catalyst.

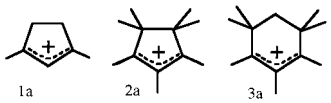

Closely related work on the aluminosilicate zeolite HZSM-5 showed that methylbenzenes are synthesized in a mechanism that passes through cyclopentenyl carbenium ions, most typically the 1,3-dimethylcyclopentenyl cation **1a**.[4] Cyclopentenyl cations were proposed to be organic reaction centers for MTO chemistry through a mechanism involving deprotonation to neutral, cyclic dienes. On HSAPO-34 we imagine an analogous mechanism in which neutral methylbenzenes are in equilibrium with benzenium cations similar to a species recently identified on HZSM-5.[5] Cation **1a** forms on HZSM-5 with very high selectivity from either ethylene, propene, or methanol as a starting material,[4,6,7] and it is indefinitely persistent at room temperature. In contrast, in the study of HSAPO-34[3] we did not observe any NMR signals that we could confidently assign to carbenium ions, even though methylaromatics readily formed.

Our failure to observe cyclopentenyl cations on HSAPO-34 raised a number of questions about the relative acid strengths of HSAPO-34 and HZSM-5 as well as the generality of our claim that methylaromatics form through cyclopentenyl cation intermediates on solid acids. We therefore explored other synthetic routes to persistent carbenium ions in this catalyst. Procedures that previously formed robust signals due to cation **1a** on HZSM-5 did indeed form very low intensity signals on HSAPO-34, but small signals make for weak evidence and suggest that only a fraction of the acid sites are sufficiently strong to sustain these cations. We were successful when we

[†] University of Southern California.

[‡] Pacific Northwest National Laboratory. Present address: Genentech, Inc., 1 DNA Way, South San Francisco, CA 94080.

10.1021/jp0041407 CCC: $20.00
Published on Web 04/19/2001

turned to acetone as a precursor. The isotropic ^{13}C chemical shifts of [2-^{13}C]acetone on HSAPO-34 do indeed show that most acid sites on this material are weaker than those on HZSM-5[8] and that a few percent are stronger. When samples of acetone on HSAPO-34 were heated in sealed MAS NMR rotors, we observed robust signals unmistakably due to a cyclopentenyl carbenium ion with an unusual substitution pattern, probably the heptamethylcyclopentyl cation **2a**. Theoretical chemical shift calculations at the GIAO-MP2/tzp/dz level[9] supported this assignment for most of the signals, but there was an appreciable discrepancy for C_4 and C_5, where the C_4–C_5 bond distance is predicted (B3LYP) to be lengthened by steric repulsion. While the analogous carbons were in better agreement with the predictions for a less-crowded heptamethylcyclohexenyl cation **3a**, the characteristic, more upfield C_1 and C_3 shift for cyclohexenyl cations, reproduced theoretically, ruled out this assignment.

We outline the mechanism by which cation **2a** could form from acetone in HSAPO-34. We also present theoretical calculations of proton affinities of parent olefins that suggest why **2a** could form to a greater extent than **1a** on this catalyst. On HSAPO-34, cyclopentenyl cations are indeed intermediates in the formation of methylbenzenes.

Experimental Section

Materials and Reagents. HSAPO-34 was prepared according to ref 10. X-ray diffraction (XRD) showed a pure crystalline phase with the CHA structure. The product was calcined at 873 K for 10 h to remove the template agent and pressed into 10−20 mesh pellets. The Brønsted site concentration was determined to be 1.1 mmol/g by elemental analysis and this was verified by acetone NMR titrations. In typical experiments 0.3 g of catalyst was activated at 673 K under 600 sccm He flow for 2 h immediately prior to use in a pulse−quench reactor. [2-^{13}C]-Acetone (% ^{13}C) and [1,3-$^{13}C_2$]acetone were obtained from Cambridge Isotopes, Inc.

Catalysis Experiments. CAVERN experiments were performed as described previously.[8,11,12] For each experiment we activated ca. 300 mg of calcined HSAPO-34 in the shallow-bed CAVERN at 723 K for 1 h to remove water. Acetone (0.38 mmol) was adsorbed at room temperature. The rotor was then sealed in the CAVERN and transferred to the NMR probe where it was heated to progressively higher temperatures followed by spectral acquisition at room temperature.

Samples were also prepared by use of a pulse−quench reactor[7,13] in a single-pulse configuration. For each experiment we loaded the reactor with a cylindrical bed (7.5 mm diameter by 8 mm in length, typical weight 300 mg) of fresh HSAPO-34 pellets. In every case, the catalyst bed was activated in place immediately prior to use by heating 1 h in flowing helium and then equilibrating at the desired reaction temperature. Previous studies have shown that the temperature of the catalyst pellets decreases 150 K in the first 170 ms of a quench. After quenching of each reacted catalyst sample, the reactor was sealed off and transferred into a glovebox filled with nitrogen. The catalyst pellets were ground and transferred to a 7.5-mm MAS rotor, which was sealed with a Kel-F end-cap similar to that used in the CAVERN studies.

Gas Chromatography. A Hewlett-Packard Model 6890 gas chromatograph with flame-ionization detector was used to analyze gases sampled from the reactor product streams through a Valco valve. The column was 150 m dh150 (Supelco) operated isothermally at 323 K to permit sampling of the gas stream more frequently than the total analysis time for any given sample. Acetic acid did not elute from the column under these conditions.

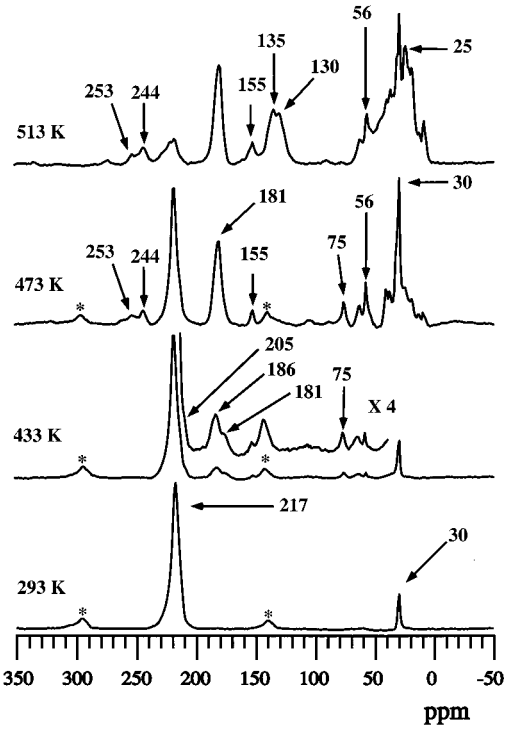

Figure 1. ^{13}C CP/MAS NMR spectra (75.4 MHz) from a CAVERN study of [2-^{13}C]acetone (1 equiv) on HSAPO-34. The sample was heated in the MAS rotor to progressively higher temperatures, as indicated, and then spectra of the reaction products in the catalyst were measured near 298 K. An asterisk denotes a spinning sideband.

NMR Spectroscopy. ^{13}C solid-state NMR experiments were performed with magic-angle spinning (MAS) on a modified Chemagnetics CMX-300 MHz spectrometer operating at 75.4 MHz for ^{13}C. Hexamethylbenzene (17.4 ppm) was used as an external chemical shift standard, and all ^{13}C chemical shifts are reported relative to TMS. Chemagnetics-style pencil probes spun 7.5 mm zirconia rotors at typically 6.5 kHz with active spin speed control (± 3 Hz).

Typical ^{13}C experiments included cross polarization (CP, contact time = 2 ms, pulse delay = 1 s, 4000 transients); cross polarization with interrupted decoupling (contact time = 2 ms, pulse delay = 1 s, 4000 transients, dipolar dephasing time of 50 μs); and single pulse excitation with proton decoupling (Bloch decay, pulse delay = 10 s, 400 transients).

Theoretical Details. The geometries of the three carbenium ions (**1a**−**3a**) and their parent olefins were studied by density functional theory (DFT). In each case the molecules were fully optimized with the hybrid B3LYP exchange-correlation functional[14] and the 6-311G* basis set. Analytic frequency calculations were done to verify that all species were minima on the potential energy surface and to obtain the thermodynamic data needed for the determination of enthalpies. The ^{13}C NMR chemical shifts were calculated at the MP2 level by the GIAO method.[9] For the NMR calculations we used a polarized triple-ζ basis set on the carbons and a double-ζ basis set on hydrogens.[15] We will refer to this basis set as tzp/dz. The reported ^{13}C chemical shifts are relative to those of the chemical shift standard TMS, obtained by the same computational procedures. We used Gaussian98[16] for all of the calculations.

Results

CAVERN Experiments. Figure 1 reports ^{13}C CP/MAS spectra from a CAVERN study of 1 equiv of [2-^{13}C]acetone on

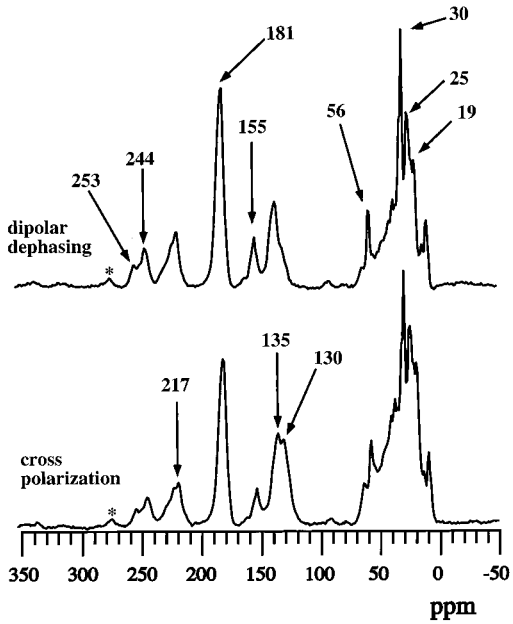

Figure 2. ^{13}C CP/MAS NMR spectra **(**75.4 MHz) showing the effects of dipolar dephasing (50 μs) on the spectrum from Figure 1 of [2-^{13}C]-acetone on HSAPO-34 after heating to a maximum of 513 K. Spectra were measured at 298 K. The essential observation is that the signals at 244−253 ppm, 155 ppm, and especially 56 ppm survive dipolar dephasing, supporting the assignment to cation **2a**. Dipolar dephasing also shows that most of the aromatic carbons are substituted and that the reaction products are rich in methyl groups. An asterisk denotes a spinning sideband.

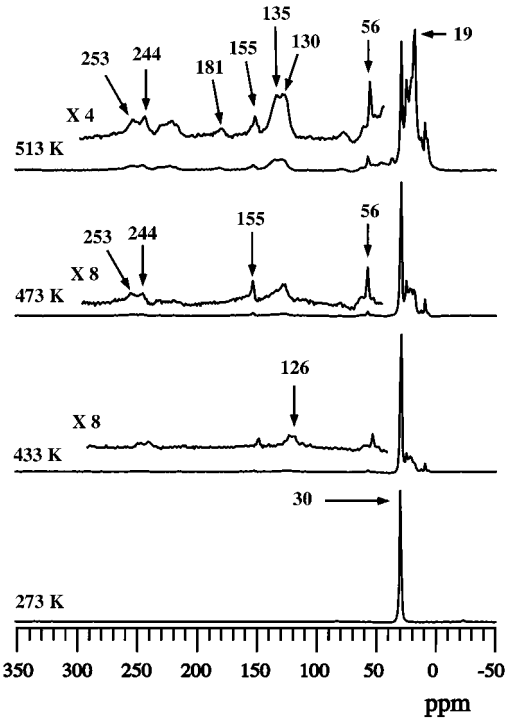

Figure 3. ^{13}C CP/MAS NMR spectra **(**75.4 MHz) from a CAVERN study of [1,3-$^{13}C_2$]acetone (1 equiv) on HSAPO-34. The sample was heated in the MAS rotor to progressively higher temperatures, as indicated, and then spectra of the reaction products in the catalyst were measured near 298 K.

HSAPO-34. This loading corresponds to 1.1 mmol/g and approximately one molecule per cage. In each case the NMR spectrum was measured near room temperature following heating of the sample rotor in the probe for ca. 20 min at progressively higher temperatures, as indicated in the figure. The spectrum acquired prior to heating (293 K) shows that most of the acetone was shifted downfield to 217 ppm as a result of hydrogen bonding to the Brønsted sites in the catalyst.[8,17] In expanded views (not shown) a small shoulder can be discerned at ca. 226 ppm. The resonance at 30 ppm is due to other isotopomers of acetone. After heating to 433 K, small signals were observed due to dimeric diacetone alcohol (75 ppm) and its dehydration product mesityl oxide (186 and 205 ppm).[8] A small resonance due to acetic acid is also apparent at 181 ppm. Significantly greater conversion of acetone to these products was achieved after heating to 473 K. In addition, small signals were also observed at 244−253, 155, and 56 ppm; their assignment to cation **2a** and the significance of this species is central to this paper. Conversion of acetone was complete after heating to 513 K. This final spectrum shows the formation of a significant amount of methylaromatics. The resonance at 135 ppm is due to substituted aromatic carbons, while the shoulder at 130 ppm is assigned to unsubstituted aromatic carbons. Integration by spectral simulation suggests an average of four substituents per ring. Methyl groups on the benzene rings are seen at 19 ppm. The above assignments are also consistent with Bloch decay spectra (not shown).

Figure 2 compares the CP/MAS spectrum of [2-^{13}C]acetone after heating at 513 K with the dipolar dephasing (interrupted decoupling) spectrum of the same sample. Of particular interest are the signals at 244−253, 155, and 56 ppm, which all survive dipolar dephasing and hence are emphasized in this spectrum. For rigid molecules, neither CH nor CH_2 carbon resonances are seen in dipolar dephasing spectra. Figure 2 also supports the finding that the aromatics formed from acetone in the HSAPO-34 cages are highly substituted, as ca. $^2/_3$ of the aromatic signal survives dipolar dephasing.

A CAVERN study of [1,3-$^{13}C_2$]acetone is reported in Figure 3. Since many of the ^{13}C labels from the methyl groups in acetone ended up as methyl groups in various products with similar chemical shifts, Figure 3 is generally less informative than Figure 1. After heating to 433 K, a small signal was seen at 126 ppm due to C_3 of mesityl oxide. Some of the label also found its way into the aromatic carbons as well as the signals at 244−253, 155, and 56 ppm.

Pulse−Quench Studies. Figure 4 reports ^{13}C CP/MAS spectra of samples prepared in a pulse−quench reactor[7,13] at various temperatures as indicated on the figure. In each case ca. 300 mg of fresh catalyst was activated in the reactor at 723 K and then equilibrated at the desired reaction temperature prior to injection of 16 μL of [2-^{13}C]acetone. In each case acetone reacted on the catalyst for 4 s with continuous product removal by He flow, and then the catalyst temperature was reduced to near ambient by a rapid thermal quench. ^{13}C CP/MAS spectra were measured at room temperature. GC analysis showed that most of the acetone passed through the catalyst without conversion within the temperature range studied; however, some acetone was retained, unreacted, on the catalyst and gave rise to the peak at 217 ppm that was also seen in the CAVERN study. Remarkably, we also saw a peak at 226 ppm with a large *relative* intensity, indicating that acetone is adsorbed more strongly to this site than to that responsible for the 217 ppm resonance. Aromatics were also trapped in the HSAPO-34 cages in the samples prepared under flow conditions, but these were substituted to a lesser degree at the highest temperature studied, 2.0 methyl groups per ring on average after reaction at 673 K. Figure 4 shows no evidence of the signals at 244−253, 155, and 56 ppm.

Flow Reactor Studies. A pulse−quench reactor was configured for continuous injection of acetone by replacing the

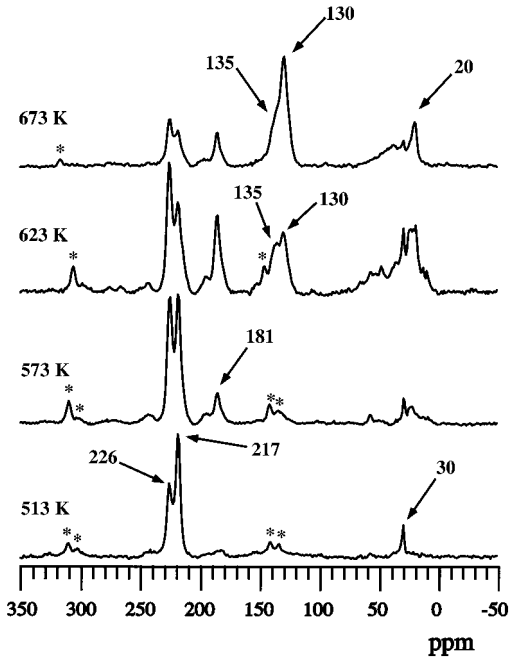

Figure 4. ^{13}C CP/MAS NMR spectra (75.4 MHz) from pulse−quench studies of [2-^{13}C]acetone on HSAPO-34. In each case a fresh catalyst bed (ca. 300 mg) was activated in place and then equilibrated at one of the temperatures shown on the figure. [2-^{13}C]Acetone (16 μL) was injected onto the catalyst bed and allowed to react for 4 s in flowing He prior to a rapid thermal quench. All spectra were measured near 298 K. The essential observation is the resolution of the 226 ppm signal from acetone on a stronger adsorption site from that at 217 ppm for acetone on a weaker adsorption site. Aromatics form at higher temperatures. An asterisk denotes a spinning sideband.

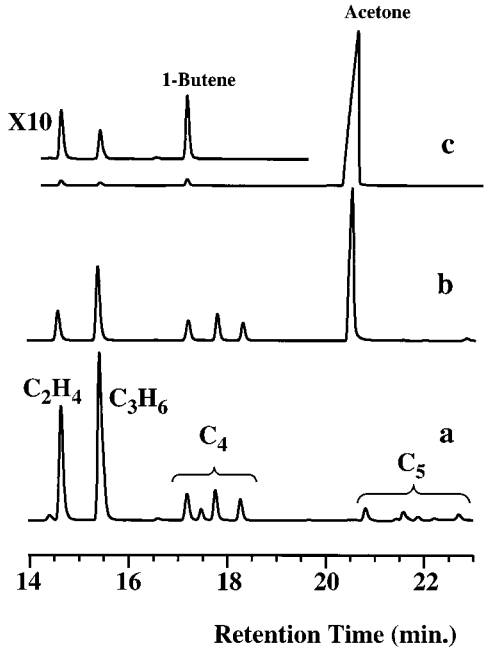

Figure 5. Gas chromatographs (FID detection) sampling the product streams of reactions carried out on HSAPO-34 catalyst beds operated at 673 K. (a) Control experiment showing activity and product selectivity with pure methanol as feed (WHSV = 8 h^{-1}). Conversion is quantitative, propene selectivity exceeds that of ethylene, and C_4 selectivity is low. (b) Pure acetone (WHSV = 8 h^{-1}), sample taken 16 min after initiating feed. Conversion is much lower than with methanol, and the C_4 (but not C_5) selectivity is clearly elevated. (c) Pure acetone (WHSV = 8 h^{-1}), sample taken 28 min after initiating feed. The catalyst is almost completely deactivated, and selectivity for both ethylene and 1-butene is elevated.

injection valve with a programmable syringe pump. Gas samples were taken periodically and analyzed by GC. Not surprisingly, the conversion of acetone on HSAPO-34 was lower than for identical experiments with methanol as a feed, and the catalyst deactivated far more rapidly, even when the acetone was diluted to 50% (v/v) with water. Nevertheless, the product selectivity from acetone was insightful. Figure 5a shows a representative GC trace from the conversion of methanol on HSAPO-34 at 673 K (WHSV = 8 h^{-1}).[18] This measurement was taken on a working catalyst, after a very short induction period, but well before deactivation. Methanol (and dimethyl ether) were almost entirely converted to hydrocarbons in this "control experiment"—the yield of propene was greater than that of ethylene, and the selectivity for C_4 products was low.

Spectra b and c in Figure 5 are from an otherwise identical study of the conversion of pure acetone (WHSV = 8 h^{-1}). The sample for chromatogram b was taken only 16 min after the acetone flow began. The ethylene/propene ratio was similar to that obtained during methanol conversion on a working catalyst, but with acetone a much higher C_4 selectivity was seen early in the life of the catalyst. The catalyst rapidly deactivated; Figure 5c is the analysis of a gas sample taken 28 min after commencing the acetone flow. Total conversion was decreased by a factor of ca. 10 in spectrum c compared to spectrum b. In Figure 5c, all C_4 products were greatly reduced on the partially deactivated catalyst with the exception of 1-butene, which was only slightly reduced. As deactivation reduced the conversion of acetone, the ethylene/propene ratio increased.

Theoretical Chemical Shifts for the Heptamethylcyclopentenyl Cation 2a. Three carbenium ions that could potentially be responsible for the observed NMR data were theoretically considered. The B3LYP/6-311G* optimized geometries of these

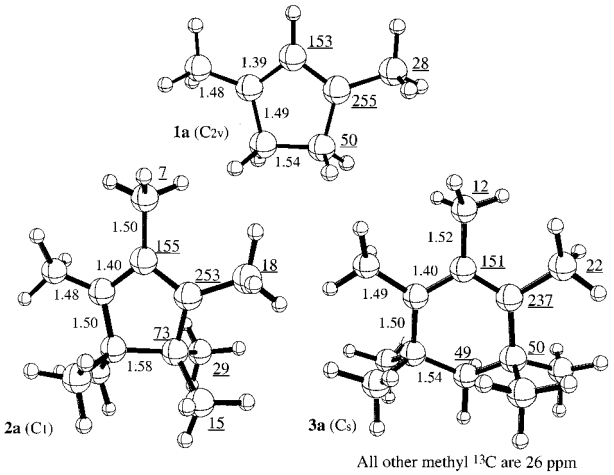

Figure 6. B3LYP/6-311G* optimizied geometries for cations **1a**−**3a**. Selected symmetry-distinct C−C bond lengths (in angstroms) are shown in smaller type. Predicted MP2-GIAO/tzp/dz//B3LYP/6-311G* ^{13}C NMR chemical shifts for symmetry-distinct atoms are shown in larger, underlined type.

are given in Figure 6. Symmetry-distinct C−C bond distances are shown, as are the ^{13}C chemical shifts, which are discussed below. We have presented the optimized geometry and NMR data for the 1,3-dimethylcyclopentadienyl cation (**1a**) in previous work.[4] We confirmed the presence of this cation during MTO and MTG chemistry on HZSM-5. Cation **1a** has C_{2v} symmetry. The delocalized nature of the positive charge is evident by the C_1–C_2 and C_2–C_3 bond lengths of 1.39 Å, intermediate between those of pure single and double bonds. On HSAPO-34, the dipolar dephasing experiment implies that the cyclopentadienyl

framework becomes completely methylated. Thus, the optimized geometry of the heptamethylcyclopentadienyl cation **2a** is also shown in Figure 6. The steric repulsion between the eclipsed methyl groups in the 4 and 5 positions causes significant distortion of the ring, which is essentially planar in cation **1a**. Although cation **2a** has C_1 symmetry, this is only due to the hydrogens on the methyl group in the 2 position. If these are ignored, the carbon skeleton has C_2 symmetry. To simplify the graphics, we assume C_2 symmetry in the presentation on the bond length and NMR data in Figure 6. Comparing **1a** and **2a**, the only significant geometric difference is in the C_4–C_5 bond length. This bond is 0.04 Å longer in **2a** than in **1a**, consistent with the steric crowding of the eclipsed methyl groups. For reasons that will be apparent when we discuss the theoretical shifts, we also considered the 1,2,3,4,4,6,6-heptamethylcyclohexadienyl cation **3a**. This carbenium ion contains the same methyl-substituted allylic substructure as cations **1a** and **2a**. Steric clashes are reduced in **3a** by the additional methylene in the 5 position. The NMR signal from this methylene could potentially be lost in the peaks from the various methyl groups. The calculated bond lengths in **3a** are very similar to those in **1a**.

GIAO-MP2/tzp/dz theoretical ^{13}C isotropic shifts for cations **1a**, **2a**, and **3a** are also reported in Figure 6. The shifts of cation **1a** have been commented on previously;[4] we focus here on the differences between the three cations. Predicted ^{13}C NMR chemical shifts for symmetry-distinct atoms are shown in larger, underlined type in Figure 6. The NMR shift of C_2 is relatively constant, varying between 151 and 155 ppm for the three cations. The chemical shift of the C_1 and C_3 carbons is similar for **1a** and **2a** (253 and 255 ppm, respectively) but much different for **3a** (237 ppm). Finally, the C_4 and C_5 carbons in **1a** and **3a** have the same shift (50 ppm), whereas it is shifted downfield to 73 ppm for **2a**.

Discussion

Relative Acid Strength of HSAPO-34. The acid strength of aluminosilicate zeolties[19] has been a contentious issue in the literature. While most workers would agree that zeolites are not superacids, well-founded differences of opinion remain about the merits of various methods for measuring acid strengths and the relative strengths of diverse solid acids. The ^{13}C isotropic shift of [2-^{13}C]acetone is commonly applied as one operational measure of acid strength,[8] and this effect has been explored theoretically.[17] The acetone shift is influenced by adsorption on either Lewis or Brønsted sites. Figures 1 and 2 show that most adsorption sites in our samples of HSAPO-34 induce an acetone shift of 217 ppm. Our interpretation is that most Brønsted acid sites in HSAPO-34 are effectively weaker than those in HZSM-5. Preliminary calculations indicate that meaningful theoretical modeling of either the deprotonation energy of an acid site in HSAPO-34 or the adsorption of acetone in this material would require a periodic treatment of an entire cage. We have not yet attempted such calculations. The acetone probe would measure a lower acid strength if the deprotonation energy of HSAPO-34 were indeed lower than for HZSM-5, but it is also possible that the small size of the SAPO-34 nanocage could prevent the most favorable hydrogen-bonding geometry and hence the largest acetone shift. The small peak at 226 ppm, which corresponds to a few percent of the total acid sites, does imply an acid strength for a minority site that is stronger than even those in HZSM-5. We searched for spectroscopic evidence of Lewis sites without success; for example, the ^{27}Al spectrum showed no extraframework aluminum. Future studies of HSAPO-34 materials of diverse origin and composition will be needed before the 226 ppm signal can be assigned to a specific structural feature.

Assignment of the 244−253, 155, and 56 ppm Signals to the Heptamethylcyclopentenyl Cation 2a. The 1,3-dimethyl and 1,2,3-trimethylcyclopentenyl cations have been identified in numerous NMR studies of microporous solid acids dating back to 1989.[6] The most easily seen resonance for these cations is a signal near 48 ppm that does not survive dipolar dephasing; this is due to C_4 and C_5, which were invariably unsubstituted (methylene) carbons in all previous studies. For the previously observed di- and trimethyl cations, C_1 and C_3 are in the vicinity of 247−250 ppm. These signals are sometimes broad or show evidence of structure, as here, and this has been interpreted as evidence of interaction with the zeolite framework.[4] For the dimethyl cation C_2 is near 147 ppm and does not survive dipolar dephasing; it is near 155 ppm for the trimethyl cation and does survive dephasing.

Like the analogous resonances for the other cylopentenyl cations, the 244−253, 155, and 56 ppm signals here always appear as a constellation and must be from the same species. This combination of chemical shifts is uniquely characteristic of a cyclopentenyl cation. The signal at 56 ppm is quite far downfield of the 48 ppm resonance previously seen for less highly substituted cations. The observation that this signal also survives dipolar dephasing can be explained, for a cyclopentenyl cation, only by disubstitution on carbons C_4 and C_5. Substitution would also tend to shift this resonance downfield, as observed. If the substituents on these carbons were diverse, the 56 ppm resonance would be broad; it is instead very sharp, suggesting that the substituting groups on all cations are identical. The dipolar dephasing spectrum in Figure 2 shows that nearly all of the upfield signal intensity is from methyl groups, and the substituents are so assigned.

In **2a** the theoretical chemical shifts for C_1 and C_3 and for C_2 are in excellent agreement with experimental values, whereas the predicted shift for C_4 and C_5 is not. Although theory predicts that C_4 and C_5 in **2a** will resonate downfield of the analogous carbons in **1a**, consistent with the experimental result, the predicted value overshoots this downfield shift by 17 ppm, a large difference. In previous studies we have compared theoretical GIAO-MP2 ^{13}C shifts with experimental results for many carbenium, oxonium, and related cations,[4,5,20−22] and in no case did we observe a difference this large. Because of this discrepancy, we also considered an alternative assignment for the NMR signals: the heptamethylcyclohexenyl cation **3a**. In this alternative structure steric repulsion between the two pairs of methyl groups is negligible, and this is reflected in normal C_4−C_5 and C_5–C_6 single bond lengths. The theoretical shift of C_4 and C_6 of cation **3a** is 50 ppm, the same as predicted for analogous carbons in **1a**. Thus, although the theoretical shift is in closer agreement with the experimental value of 56 ppm, the theoretical methods do not predict the downfield shift observed experimentally. In addition, whereas the value for C_2 (151 ppm) is in reasonable agreement, the value for C_1 and C_3 (237 ppm) deviates significantly from experiment. Indeed, the theoretical shifts for cation **3a** are in excellent agreement with experimental values for cyclohexenyl cations, and we must look elsewhere to explain the discrepancy between the experimental and theoretical shift of C_4 and C_5 of cation **2a**. It is possible that the large, heavily substituted cation is sterically hindered by the SAPO-34 cage, which alters its geometry from that which we calculate free from the zeolite. Furthermore, the cation may interact closely with the zeolite conjugate base site, which could

SCHEME 1

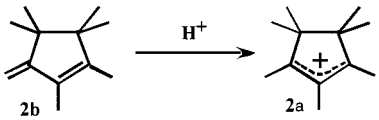

also result in differences in chemical shift. Although the theoretical results are less telling than we have come to expect, they still support the assignment of the cyclopentenyl cation signals to species **2a**.

Significance of the Heptamethylcyclopentenyl Cation 2a. This is the first reported observation of any persistent carbenium ion in a SAPO material. In unpublished experiments we have observed very low concentrations of other carbenium ions in HSAPO-34. Low-intensity signals from the 1,3-dimethylcyclopentenyl cation were observed in some pulse−quench work with propene, but these results were not compelling. Here, the 244−253, 155, and 56 ppm signals are at least comparable to those in the first reports of various cations in aluminosilicate zeolites, and the claim of a persistent cation in HSAPO-34 can be made with confidence. The cation observed here is also the first cyclopentenyl cation with subtituents on C_4 and C_5 characterized on any microporous solid acid.

In previous work we have shown that the presence of persistent carbenium ions in aluminosilicate zeolites requires that the parent aromatic or olefin be highly basic.[23] Specifically, we found that only those aromatics or olefins with proton affinities (enthalpies) greater than ∼209 kcal/mol would form persistent carbenium ions on aluminosilicate zeolites. This concept is illustrated in Scheme 1, which depicts protonation of the exocyclic diene **2b** to form carbenium ion **2a**. Note that **2b** is the only olefin that affords cation **2a** in an elementary protonation step without oligomerization or skeletal isomerization, and no olefin can be formulated with two endocyclic double bonds as a result of the substitution pattern on C_4 and C_5. Figure 7 reports the theoretical geometries of the neutral dienes **1b**, **2b**, and **3b** that give rise to the corresponding cations by protonation. Olefin **3b** also has an exocyclic double bond, conforming to the same restrictions as **2b**. All three structures show C−C bond lengths consistent with expected bond orders and conjugation.

As mentioned above, persistent carbenium ions are expected to form on aluminosilicate zeolites if the proton affinities of the parent olefins are greater than 209 kcal/mol. At the B3LYP/6-311G* level of theory, the proton affinities of **1b**, **2b**, and **3b** are 222.4, 227.6, and 226.6 kcal/mol, well above our previously reported threshold. However, while we know that DFT usually gives a reasonable prediction of the geometries of the cations and their parent olefins, DFT does not give a good prediction of the proton affinities. In previous work[23] we found that we need higher order correlation, specifically MP4(sdtq)/6-311+G*, to obtain reasonable values. At the MP4(sdtq)/6-311+G*//B3LYP/TZVP level of theory the proton affinity of **1b** is 215.6 kcal/mol, about 7 kcal/mol lower than the B3LYP/6-311G* value. While we did not attempt the much more computationally expensive MP4 proton affinity calculations for **2b** and **3b**, we expect the difference between the two levels of theory to be similar. Thus, even after adjustment, all three olefins are sufficiently basic to form persistent carbenium ions in aluminosilicate zeolites.

However, when we attempted to form cation **1a** in HSAPO-34 using methods that produce robust NMR signals in zeolite HZSM-5, we saw either no signals at all or weak signals of slight regard. Given that acetone reports that most acid sites in HSAPO-34 are weaker than those on HZSM-5, it is likely that the proton affinity threshold for carbenium ion persistence is higher in HSAPO-34. Olefin **2b** is over 5 kcal/mol more basic than olefin **1b**, which likely explains the ready persistence of **2a** but not **1a** on HSAPO-34.

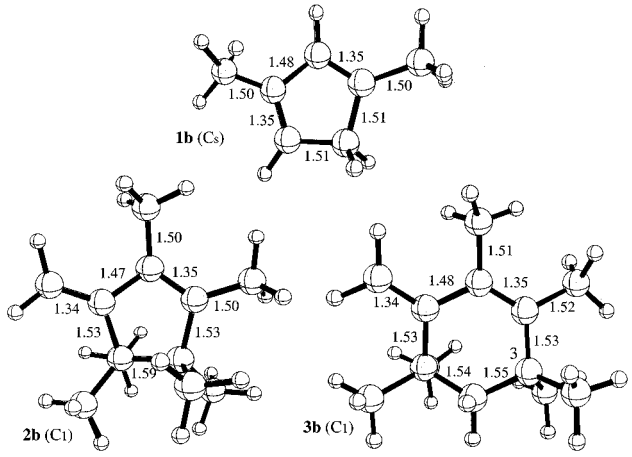

Figure 7. B3LYP/6-311G* optimizied geometry for olefins **1b**−**3b**. Selected symmetry-distinct C−C bond lengths (in angstroms) are shown in smaller type.

Reaction Mechanism for Conversion of Acetone to Aromatics on HSAPO-34. Earlier CAVERN studies of acetone on aluminosilicate zeolites[8] elucidated several reaction pathways for acetone on those materials. Acetone was shown to cyclotrimerize to the unsaturated ketone isophorone, which at higher temperatures would lose water and hydrogen to form trimethylbenzenes. Alternatively, dimeric mesityl oxide would crack in the presence of water to make acetic acid and isobutylene (which would in turn react to make other products).

Here, on HSAPO-34, we saw neither the cyclic trimer isophorone nor the linear trimer phorone. We also did not observe any CO_2, which commonly formed on the zeolites and was attributed to the cracking of phorone. Instead, we saw the formation of much more acetic acid than on any zeolite studied other than HZSM-5. These observations show that the aldol condensation of acetone on HSAPO-34 proceeds no further than mesityl oxide, all of which cracks with water to form acetic acid (which reacts no further) and isobutylene (which forms all of the hydrocarbon products).

In the CAVERN experiments we saw three major hydrocarbon products, the heptamethylcyclopentyl cation **2a**, alkanes, and heavily methylated benzenes. We believe that the very high selectivity for cation **2a** reflects the fact that this C_{12} species is made in the SAPO cages by a fairly clean trimerization of C_4 olefins, the latter produced by cracking of mesityl oxide. This contrasts with most previous routes to cylopentenyl cations in zeolites. For example, in ref 4, the 1,3-dimethylcyclopentenyl cation (a C_7 species) formed from ethylene through a complex and ill-characterized route, but here a C_{12} species apparently forms through a more-direct trimerization of C_4 olefins.

Methyl migrations and skeletal isomerizations are facile for hydrocarbons on solid acids at high temperature, and the identification of a unique mechanism for the formation of **2a** is not practical, but Scheme 2 is offered as a representative pathway.

In HSAPO-34, acetone is converted to acetic acid and isobutylene. The latter is not capable of leaving (or entering) the cages in HSAPO-34. We verified this by flowing pure isobutylene over a bed of HSAPO-34 at 723 K. There was no conversion whatsoever, and even after prolonged exposure the

SCHEME 2

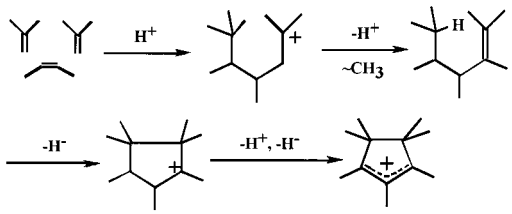

catalyst contained no detectable carbon. However, isobutylene can isomerize in the cages to linear butenes, which, as Figure 5 demonstrates, exit the catalyst in appreciable amounts when acetone is flowed over fresh catalyst. Scheme 2 suggests trimerization of two isbutylenes and one molecule of 2-butene followed by a straightforward methyl migration to set up the correct carbon skeleton for ring closure. The loss of 2 equiv of H_2 in the passage from C_4 olefins to cation **1** requires that two other olefin molecules be reduced to alkanes by proton transfer and hydride abstraction steps. Indeed, much of the upfield signal intensity in Figures 1−3 is accounted for by alkanes (for a well-resolved example, note the peak at 9 ppm, which is characteristic of one carbon type in a number of highly branched alkanes).

Conversion of cation **2a** ($C_{12}H_{21}^+$) to hexamethylbenzene ($C_{12}H_{18}$) requires loss of a final equivalent of H_2 (by reduction of another olefin molecule) and transfer of a proton back to the acid site. As pointed out previously,[23] the proton affinity of hexamethylbenzene (205.7 kcal/mol) is below the threshold for formation of a persistent carbenium ion on aluminosilicate zeolites. Reference 4 detailed the steps and theoretical energetics for the conversion of the 1,3-dimethylcyclopentenyl cation to toluene. A key step in that pathway was hydride abstraction from a ring carbon of C_7H_{10} to form a tertiary carbenium ion. We note that the heptamethylcyclopentenyl cation has no hydrogens on ring carbons, and an analogous hydride abstraction from olefin **2b** would necessarily occur on a methyl group to yield (formally) a primary carbenium ion. The energetic difficulty of this hydride abstraction step may contribute to the high yield of cation **2a** in Figures 1−3.

While the present study is further evidence for the intermediacy of cyclopentenyl cations in the formation of methylaromatics, it may be that cation **2a** will more readily lose hydrogen after transferring one methyl group to either another organic species or to the catalyst framework. Thus, we might expect to see the formation of benzenes with fewer than six methyl groups, and an average number of 4 was indeed estimated from Figures 1 and 2.

Relevance of This Study to Methanol-to-Olefin Catalysis. We recently proposed that methylbenzenes are part of the active site for olefin synthesis on HSAPO-34.[3] These form during the kinetic induction period and undergo side-chain methylation to yield ethylbenzene and cumene derivatives. Alternatively, highly methylated benzenes can rearrange to extend alkyl chains. Either way, these species generate the primary olefinic products. Here we have shed some light on the formation of methylbenzenes and demonstrated that cyclopentenyl cations can indeed form on HSAPO-34 under conditions that also form methylbenzenes.

While acetone does react to form methylbenzenes on HSAPO-34, and these apparently eliminate ethylene and propene (Figure 5b), acetone cannot remethylate the aromatics to form a complete catalytic cycle. Instead, isobutylene from cracking of mesityl oxide forms additional aromatics until all pores are full and the catalyst is deactivated. This occurs rapidly. Note that as the catalyst becomes almost completely deactivated, the ethylene selectivity increases (Figure 5c), by itself a desirable property. We speculate that the last olefinic products formed on the deactivating catalyst are eliminated from benzene rings that have already lost most of their substituents, and rings capable of eliminating ethylene outnumber those that can eliminate propene.

Acetone conversion also differs from methanol conversion in the high initial selectivity for C_4 olefins obtained with the former. In Figure 5b, the total C_4 selectivity exceeds that of C_2 and C_4, while it does not with methanol as a feed (cf. Figure 5a). Yet, the C_5 selectivity with methanol exceeds that with acetone. This is a reflection of the primacy of isobutylene as a hydrocarbon product of acetone and its isomerization to linear products, which escape the HSAPO-34 cages.

Acknowledgment. J.F.H. is supported by the National Science Foundation (CHE-9996109) and the U.S. Department of Energy (DOE) Office of Basic Energy Sciences (BES) (Grant DE-FG03-93ER14354). J.B.N. is funded by the Department of Energy (DOE) Office of Science. Computer resources were provided by the National Energy Research Supercomputer Center (NERSC), Berkeley, CA, and the National Center for Supercomputing Applications (NCSA). Pacific Northwest National Laboratory is a multipurpose national laboratory operated by Battelle Memorial Institute for the U.S. DOE.

References and Notes

(1) Stöcker, M. *Microporous Mesoporous Mater.* **1999**, *29*, 3−48.
(2) Wilson, S.; Barger, P. *Microporous Mesoporous Mater.* **1999**, *29*, 117−126.
(3) Song, W.; Haw, J. F.; Nicholas, J. B.; Heneghan, K. *J. Am. Chem. Soc.* **2000**, *122*, 10726−10727.
(4) Haw, J. F.; Nicholas, J. B.; Song, W. G.; Deng, F.; Wang, Z. K.; Xu, T.; Heneghan, C. S. *J. Am. Chem. Soc.* **2000**, *122*, 4763−4775.
(5) Xu, T.; Barich, D. H.; Goguen, P. W.; Song, W.; Wang, Z.; Nicholas, J. B.; Haw, J. F. *J. Am. Chem. Soc.* **1998**, *120*, 4025−4026.
(6) Haw, J. F.; Richardson, B. R.; Oshiro, I. S.; Lazo, N. L.; Speed, J. A. *J. Am. Chem. Soc.* **1989**, *111*, 2052−2058.
(7) Goguen, P. W.; Xu, T.; Barich, D. H.; Skloss, T. W.; Song, W.; Wang, Z.; Nicholas, J. B.; Haw, J. F. *J. Am. Chem. Soc.* **1998**, *120*, 2651−2652.
(8) Xu, T.; Munson, E. J.; Haw, J. F. *J. Am. Chem. Soc.* **1994**, *116*, 1962−1972.
(9) Gauss, J. *Chem. Phys. Lett.* **1992**, *191*, 614−620.
(10) Lok, B. M.; Messina, C. A.; Patton, R. L.; Gajek, R. T.; Cannan, T. R.; Flanigen, E. M. U.S. Patent 4,440,871, 1984.
(11) Munson, E. J.; Murray, D. K.; Haw, J. F. *J. Catal.* **1993**, *141*, 733−736.
(12) Xu, T.; Haw, J. F. *Top. Catal.* **1997**, *4*, 109−118.
(13) Haw, J. F.; Goguen, P. W.; Xu, T.; Skloss, T. W.; Song, W.; Wang, Z. *Angew. Chem.* **1998**, *37*, 948−949.
(14) Becke, A. D. *J. Chem. Phys.* **1993**, *98*, 5648−5652.
(15) Schafer, A.; Horn, H.; Ahlrichs, R. *J. Chem. Phys.* **1992**, *97*, 2571−2577.
(16) Frisch, M. J.; Trucks, G. W.; Schlegal, H. B.; Gill, P. M. W.; Johnson, B. G.; Robb, M. A.; Cheeseman, J. R.; Keith, T.; Petersson, G. A.; Montgomery, J. A.; Raghavachari, K.; Al-Laham, M. A.; Zakrzewski, V. G.; Ortiz, J. V.; Foresman, J. B.; Cioslowski, J.; Stefanov, B. B.; Nanayakkara, A.; Challacombe, M.; Peng, C. Y.; Ayala, P. Y.; Chen, W.; Wong, M. W.; Andres, J. L.; Replogle, E. S.; Gomperts, R.; Martin, R. L.; Fox, D. J.; Binkley, J. S.; Defrees, D. J.; Baker, J.; Stewart, J. P.; Head-Gordon, M.; Gonzalez, C.; Pople, J. A. *Gaussian 94*, Revision B.2.; Gaussian, Inc.: Pittsburgh, PA, 1995.
(17) Barich, D. H.; Nicholas, J. B.; Xu, T.; Haw, J. F. *J. Am. Chem. Soc.* **1998**, *120*, 12342−12350.
(18) Weight hourly space velocity (WHSV) formally has units of grams of reactant per gram of catalyst per hour.
(19) Haw, J. F.; Nicholas, J. B.; Xu, T.; Beck, L. W.; Ferguson, D. B. *Acc. Chem. Res.* **1996**, *29*, 259−267.
(20) Nicholas, J. B.; Xu, T.; Barich, D. H.; Torres, P. D.; Haw, J. F. *J. Am. Chem. Soc.* **1996**, *118*, 4202−4203.
(21) Xu, T.; Barich, D. H.; Torres, P. D.; Haw, J. F. *J. Am. Chem. Soc.* **1997**, *119*, 406−414.
(22) Xu, T.; Barich, D. H.; Torres, P. D.; Nicholas, J. B.; Haw, J. F. *J. Am. Chem. Soc.* **1997**, *119*, 396−405.
(23) Nicholas, J. B.; Haw, J. F. *J. Am. Chem. Soc.* **1998**, *120*, 11804−11805.